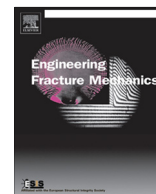




ELSEVIER

Contents lists available at ScienceDirect

Engineering Fracture Mechanics

journal homepage: www.elsevier.com/locate/engfracmech

Interlaminar fracture toughness of glass and carbon reinforced multidirectional fiber metal laminates

Jarosław Bieniaś*, Konrad Dadej, Barbara Surowska

Department of Materials Engineering, Faculty of Mechanical Engineering, Lublin University of Technology, Nadbystrzycka 36, 20-618 Lublin, Poland

ARTICLE INFO

Article history:

Received 11 August 2016

Received in revised form 8 February 2017

Accepted 9 February 2017

Available online xxx

Keywords:

Asymmetric end notch flexure

Interlaminar fracture toughness

Fiber metal laminates

Cohesive Zone Analysis

Fiber orientation

ABSTRACT

CARALL and GLARE type multidirectional fiber metal laminates were subjected to interlaminar fracture toughness tests by End Notched Flexure method. The critical strain energy release rates were calculated based on authors developed methodology of recent analytical Enhanced Beam Theory, and then verified by standardized experimental Compliance Calibration method. With increase of fiber orientation angle (0° , 45° , 90°) at the metal-composite interface, the determined critical strain energy release rate significantly decreased. Simultaneously, the growing contribution of mode I in resulting mode mixity ratio at the crack tip was revealed. Performed experimental tests were supported by Finite Element Analysis by Cohesive Zone Method.

© 2017 Elsevier Ltd. All rights reserved.

1. Introduction

Fiber metal laminates (FMLs) are hybrid materials consisting of alternatively arranged metal layers (most frequently aluminium alloys) adhesively bonded with layers of polymer matrix composite reinforced with continuous fibers. They are characterized by enhanced mechanical properties, e.g. high strength to density ratio, high resistance to mechanical fatigue and to low velocity impact [1–4]. The GLARE (Glass Aluminium Reinforced Laminates) applied in aircraft industry are the most prevalent and most investigated type of FML laminates. Research works are also carried out in the scope of application of other metal alloys and reinforcing fibers e.g. CARALL (Carbon Aluminium Reinforced Laminates) [1].

In recent years, several papers were published about experimental Interlaminar Fracture Toughness (IFT) tests concerning metal-composite adhesive joints. In fiber metal laminates this adhesive joint was usually tested in mode I by Double Cantilever Beam (DCB) or Single Cantilever Beam (SCB) [5–9]. However, in above mentioned literature, when comparing obtained results of metal-composite joint with analogous composite materials, the determined values of critical strain energy release rates (SERR) are rather different from each other. Airoidi et al. [5] as well as Cortés and Cantwell [6] estimated SERR for metal-composite interface at similar level, as for analogous classical composite. Reyes and Cantwell [9] observed increasing value of strain energy release rate G_{Ic} with crack growth. This observation was explained by extending the bridging fibers connecting two opening surfaces. Reyes and Cantwell [9] also noted that after a certain crack length, the critical strain energy release rate G_{Ic} for metal-composite joint significantly exceeded the value determined for analogous pure composite. Similarly, Abdullah et al. [7] observed that SERR of FMLs is higher than for the analogous pure composites, suggesting that the composite has been successfully bonded to the aluminium substrate.

* Corresponding author.

E-mail address: j.bienias@pollub.pl (J. Bieniaś).<http://dx.doi.org/10.1016/j.engfracmech.2017.02.007>

0013-7944/© 2017 Elsevier Ltd. All rights reserved.

Nomenclature

$0^\circ/\varphi$	interface between composite layers with orientation 0° and φ
al/φ	interface in fiber metal laminates between aluminium layer and adjacent composite with orientation φ
α	marking of sublaminates ($\alpha \in 1,2,3$)
δ	bulk deflection recorded in end notch flexure tests
$\delta_{nn}, \delta_{ss}, \delta_{tt}$	separation in normal, first shear and second shear direction in traction – separation law
ρ_u	crack-tip sliding displacement rate
ρ_w	crack-tip opening displacement rate
ρ_ϕ	crack-tip relative rotation rate
φ	angle between specimen axis and orientation of lower layer of interface
χ	coefficient concerning the stiffness proportion of sublaminates 1 and 2
a_0	initial delamination length in end notch flexure tests
a_n	initial delamination length n in compliance experimental tests
$a_\alpha, b_\alpha, c_\alpha, d_\alpha$	equivalent compliance of sublaminates α
$A_\alpha, B_\alpha, C_\alpha, D_\alpha$	equivalent stiffness of sublaminates α
B	laminate width
C	compliance of end notch flexure specimen
dC/da	compliance differential in function of initial delamination length
dy/dx	slope of determined compliance calibration line
e_{ij}	Voigt elastic constants
E_{ij}, G_{ij}, ν_{ij}	elastic constants
$E', E_{slender}'$	equivalent elastic modulus used in the characteristic length equation for infinite body and slender bodies
$f_{uN}, f_{uM}, f_{\phi N}, f_{wQ}, f_{\phi M}$	flexibility coefficients
G	total strain energy release rate in mixed mode fracture
G_{Ic}, G_{IIc}	critical strain energy release rate in mode I and mode II
G^{EBT}, G^{CC}	critical strain energy release rate determined by EBT and CC method
h	half thickness of bulk joined by cohesive elements
h_1, h_2	half thickness of sublaminates 1 and 2
K_{nn}, K_{ss}, K_{tt}	cohesive penalty stiffness in normal, first shear and second shear direction in traction – separation law
l	half of distance between supports in ENF test fixture
$l_{ch,I}, l_{ch,II}$	cohesive zone length for mode I and mode II in infinite body
$l_{ch,slender,I}, l_{ch,slender,II}$	cohesive zone length for mode I and mode II in slender bodies
L_{cz}	cohesive zone length
$L_{cz,predicted}$	predicted cohesive zone length
L_{el}	finite element length
m	compliance parameter for energy release rate calculations
M_α	bending moments acting the crack tip segment of sublaminates 1, 2 and 3
N_α	normal force acting the crack tip segment of sublaminates 1, 2 and 3
N_{el}	number of finite elements within predicted cohesive zone length
P, P_d	downward force acting ENF specimen
Ra, Rb	reaction force of left and right supports in ENF test
Ra_1, Ra_2	components of reaction force Ra acting on sublaminates 1 and 2
t_{nn}, t_{ss}, t_{tt}	Traction stress at normal, first shear and second shear direction in traction – separation law
Q_α	shearing force acting the crack tip segment of sublaminates 1, 2 and 3
w_1, w_2	transverse displacements of crack tip point in sublaminates 1 and 2

Acronyms

ARALL	aramid aluminium reinforced laminates
BK	Benzeggagh-Kenane delamination criterion
CAA	chromium acid anodizing
CARALL	carbon aluminium reinforced laminates
CC	experimental compliance calibration
CFRP	carbon fiber reinforced polymer
CLT	classical laminate theory
CZM	cohesive zone method
DCB	double cantilever beam
EBT	enhanced beam theory
ENF	end notched flexure
FEA	finite element analysis
FML	fiber metal laminates

Download English Version:

<https://daneshyari.com/en/article/5013995>

Download Persian Version:

<https://daneshyari.com/article/5013995>

[Daneshyari.com](https://daneshyari.com)